We are IntechOpen,
the world's leading publisher of
Open Access books
Built by scientists, for scientists

6,900
Open access books available

186,000
International authors and editors

200M
Downloads

Our authors are among the

154
Countries delivered to

TOP 1%
most cited scientists

12.2%
Contributors from top 500 universities

CLARIVATE ANALYTICS

BOOK CITATION INDEX

INDEXED

WEB OF SCIENCE™

Selection of our books indexed in the Book Citation Index
in Web of Science™ Core Collection (BKCI)

Interested in publishing with us?
Contact book.department@intechopen.com

Numbers displayed above are based on latest data collected.
For more information visit www.intechopen.com

Cellular MIMO Systems

Wei Peng
Tohoku University,
Japan

1. Introduction

Multiple-input multiple-output (MIMO) has been accepted as a promising technology for its potential to achieve low bit error rate (BER) by space time coding [1] or to achieve large capacity by multiplexing [2]. MIMO multiplexing has been widely adopted to realize high speed data communications. The capacity of MIMO systems in the point-to-point transmission without external interferences has been studied in [3, 4] to show that large capacity can be achieved in a rich scattering environment. In a cellular environment, the same frequency/frequencies can be used in neighboring cells. As a result, co-channel interference exists and the channel between the base-station (BS) and the mobile-station (MS) is changed from noise-limited channel to interference-limited channel.

Recently, the capacity of MIMO systems in the cellular environment has attracted much interest. Uplink (transmission from MS to BS) capacity with variable-rate transmissions is studied in [5]. By modeling the co-channel interference as additive white Gaussian noise (AWGN), the uplink capacity is also studied in [6, 7]. On the other hand, from the users' stand point, the downlink capacity may be more interesting. However, the results for the downlink capacity of cellular MIMO systems presented in the literature are mainly based on the simulation results. Very detailed simulation results for the downlink MIMO capacity in 3G FDD WCDMA cellular systems can be found in [8]. By assuming single-frequency-reuse (the frequency reuse factor (FRF) equals to 1), the capacity of downlink cellular MIMO systems is studied by simulations and the results are presented in [9, 10]. These results are given in terms of the number of antennas, the modulation schemes, the propagation parameters as well as the cell size. However, FRFs other than 1 are not considered. By taking various FRFs into consideration, a comparative study on the capacity of cellular MIMO systems is presented in [11]. A comprehensive comparison between the capacity of SISO, SIMO, STBC-MISO and MIMO systems in a cellular environment is made based on the simulation results.

In general, fixed FRF has been considered in cellular systems. It is reported in [12] that a flexible FRF may help to improve the capacity for cellular single antenna (SISO) systems. However, flexible design of FRF for cellular MIMO systems is rarely available in the literature.

In this chapter, the downlink capacity of cellular MIMO systems is theoretically analyzed in terms of both the ergodic and outage capacities. The theoretical results of the best and worst situation capacities suggest that the greatest capacities may be achieved by using FRF 1 or FRF 3 adaptively according to the situations. Therefore, a hybrid frequency reuse scheme is

introduced to maximize the overall downlink capacity. It is shown by numerical results that the average ergodic and outage capacities can both be increased by the hybrid frequency reuse scheme when compared with the schemes using fixed FRF 1 or FRF 3. Especially, when compared with the commonly accepted FRF 1 scheme, the average outage capacity can be increased as much as 50%. Therefore, by using the hybrid frequency reuse scheme, the coverage problem of the single-frequency-reuse cellular systems can be greatly alleviated.

The rest of the chapter is organized as follows. Section 2 describes the system model of the point-to-point MIMO systems. Some useful results for the capacity of point-to-point MIMO systems are also presented. Section 3 describes the system model of the cellular MIMO systems. The currently existing frequency reuse schemes are introduced. And the ergodic and outage capacities are theoretically analyzed based on the cellular structures of different frequency reuse schemes. The hybrid frequency reuse scheme is proposed in Section 4. Numerical results are then presented in Section 5. Finally, the chapter is concluded in Section 6.

2. Point-to-point MIMO systems

A. System model

The received signal in a point-to-point MIMO system with N_t transmit and N_r receive antennas can be written as

$$\mathbf{y} = \mathbf{H}\mathbf{x} + \mathbf{n} ,\qquad(1)$$

where $\mathbf{H}$ is an $N_r \times N_t$ channel matrix. The elements of $\mathbf{H}$ are identical and independently distributed (i.i.d.) complex Gaussian variables with zero mean and unit variance (This means that we assume Rayleigh fading). $\mathbf{y}$ is the N_r – dimensional received signal vector. $\mathbf{x}$ is the N_t – dimensional transmitted signal vector. n is the N_r – dimensional additive white Gaussian noise (AWGN) vector with variance σ^2.

B. Capacity analysis for point-to-point MIMO systems

The capacity C of the MIMO systems from the view point of information theory is the mutual information between input signals and output signals, given by [13]

$$C = I\left(\mathbf{x};(\mathbf{y},\mathbf{H})\right) = E\left\{I\left(\mathbf{x};\mathbf{y}|\mathbf{H}=H\right)\right\} ,\qquad(2)$$

where $E\{\cdot\}$ represents the expectation over channel realizations and H represents the instantaneous channel matrix.

It is assumed that the receiver has perfect channel state information (CSI) but the transmitter does not. Therefore, the transmitted power is allocated equally to each transmit antenna. According to (2), the capacity for a system with N_t transmit and N_r receive antennas is generally given by [3, 4]

$$C_{MIMO} = E\left\{\log_2 \det\left(\mathbf{I}_{N_r} + \frac{P_t}{N_t\sigma^2}\mathbf{H}\mathbf{H}^*\right)\right\} ,\qquad(3)$$

where $P_t = E\left\{\|\mathbf{x}\|^2\right\}$ is the average total transmitted power and superscript $*$ represents conjugate transpose. Let $\mathbf{S} = \mathbf{HH}^*$ if $N_r < N_t$ and $\mathbf{S} = \mathbf{H}^*\mathbf{H}$ otherwise, $n = \max\{N_r, N_t\}$ and $m = \min\{N_r, N_t\}$. The capacity in (3) can be rewritten in respect of the eigenvalues $\lambda_1, \cdots, \lambda_m$ of the matrix $\mathbf{S}$ as [4]

$$C_{MIMO} = E\left\{\sum_{i=1}^{m}\log_2\left(1 + \frac{P_t}{N_t\sigma^2}\lambda_i\right)\right\}. \tag{4}$$

When the components of noise vector and transmitted signal vector are i.i.d. and $rank(\mathbf{H}) = m$, C_{MIMO} in (4) can be rewritten as [4]

$$C_{MIMO} = m\int_0^{\infty}\log_2\left(1 + \frac{P_t}{N_t\sigma^2}\lambda\right)p(\lambda)d\lambda. \tag{5}$$

Since we are assuming Rayleigh fading, the probability density function (p. d. f) of λ, $p(\lambda)$, is given by

$$p(\lambda) = \frac{1}{m}\sum_{k=0}^{m-1}\frac{k!}{(k+n-m)!}\left[L_k^{n-m}(\lambda)\right]^2\lambda^{n-m}e^{-\lambda}, \tag{6}$$

where $L_k^{n-m}(\lambda) = \frac{1}{k!}e^{\lambda}\lambda^{m-n}\frac{d^k}{d\lambda^k}\left(e^{-\lambda}\lambda^{n-m+k}\right)$.

Increasing the number of receive antennas will increase degree of freedom and therefore improve the capacity performance. However, MSs could not employ large number of antennas due to the size limitation. Therefore, in this study, the number of the receive antennas is assumed to be equal to the number of transmit antennas. Under this assumption, the capacity in (5) becomes

$$C_{MIMO} = \int_0^{\infty}\log_2\left(1 + \frac{P_t}{N_t\sigma^2}\lambda\right)\sum_{k=0}^{m-1}\left[L_k(\lambda)\right]^2e^{-\lambda}d\lambda, \tag{7}$$

where $L_k(\lambda) = \frac{1}{k!}e^{\lambda}\frac{d^k}{d\lambda^k}\left(e^{-\lambda}\lambda^k\right)$. Note that although the expression in (7) yields the ergodic capacity, the outage capacity can also be evaluated similarly. For example, the outage capacity $C_{10\%}$ (which represents an outage of 10%) can be obtained by

$$C_{10\%} = m\log_2\left(1 + \frac{P_t}{N_t\sigma^2}\lambda_{10\%}\right), \tag{8}$$

where $\lambda_{10\%}$ satisfies $P\left(\lambda < \lambda_{10\%}\right) = 0.1$.

3. Cellular MIMO downlink transmission

A. System model

In the cellular circumstance, there exists co-channel interference from the neighboring cells due to the frequency reuse. The received signal vector in (1) should be modified to include the path loss effect and shadowing loss effect as well as the co-channel interference as

$$\mathbf{y}_{cellular} = d_0^{-\alpha} 10^{-\xi/10} \mathbf{Hx} + \sum_{i=1}^{B} d_i^{-\alpha} 10^{-\xi/10} \mathbf{H}_i \mathbf{x}_i + \mathbf{n}$$
$$= d_0^{-\alpha} 10^{-\xi/10} \mathbf{Hx} + \mathbf{v}$$

(9)

In (9), d_0 represents the distance between the MS and the desired BS, $d_i (i = 1, \cdots, B)$ represents the distance between the MS and the ith co-channel BS, α represents the path loss exponent and B is the number of considered co-channel BSs; ξ represents the shadowing loss in dB, which follows the Gaussian distribution with zero mean and standard derivation σ_ξ. It is reported in [10] that the system capacity will decrease when σ_ξ increases. However, such decrease will not exceed 50% (3dB) when σ_ξ increases from 0 dB to 8 dB. To simplify the analysis, in this study, $\xi = 0$ (no shadowing loss) is assumed; $\mathbf{H}_i$ represents the channel matrix between the MS and the ith co-channel BS and $\mathbf{x}_i$ is the transmitted signal vector from the ith co-channel BS; $\mathbf{v} = \sum_{i=1}^{I} d_i^{-\alpha} \mathbf{H}_i \mathbf{x}_i + \mathbf{n}$ represents the interference plus noise term.

The co-channel interference is usually modeled as Gaussian distributed [6, 7]. Under this assumption, $\mathbf{v}$ can be treated as equivalent AWGN with zero mean and variance [14]

$$\sigma_v^2 = \text{var}\{\mathbf{v}\} = \text{var}\left\{ \sum_{i=1}^{B} d_i^{-\alpha} \mathbf{H}_i \mathbf{x}_i + \mathbf{n} \right\} = \sum_{i=1}^{B} d_i^{-\alpha} E\left\{ \|\mathbf{x}_i\|^2 \right\} + \sigma^2 ,$$

(10)

where $E\left\{ \|\mathbf{x}_i\|^2 \right\}$ is the average total transmitted power of $\mathbf{x}_i$.

B. Frequency Reuse schemes

There are two types of frequency reuse schemes where integer FRFs or non-integer FRFs are used. The non-integer FRF was recently introduced by [12]. In the following, the frequency reuse schemes with integer FRFs and non-integer FRFs will be described respectively.

a.   Frequency Reuse Scheme with Integer FRFs

Fig. 1 shows the co-channel interference from the neighboring cells to a MS in the central cell. Integer FRFs of 1, 3, 4 and 7 are used for example. Here, the best situation and the worst situation are defined according to the received signal-to-noise- ratio (SNR). The best situation happens with the MS near the center of the cell where the desired BS locates. The worst situation happens with the MS at the boundary of the cell, where the distance between the MS and the desired BS is largest [5]. Let K represent the FRF. As shown in Fig. 1, when $K \geq 3$, the co-channel interferers in the second and above tiers are far away from the MS and therefore their interference can be ignored. However, when $K = 1$, the interferers in the second tier are no more negligible. Therefore, when $K = 1$, co-channel
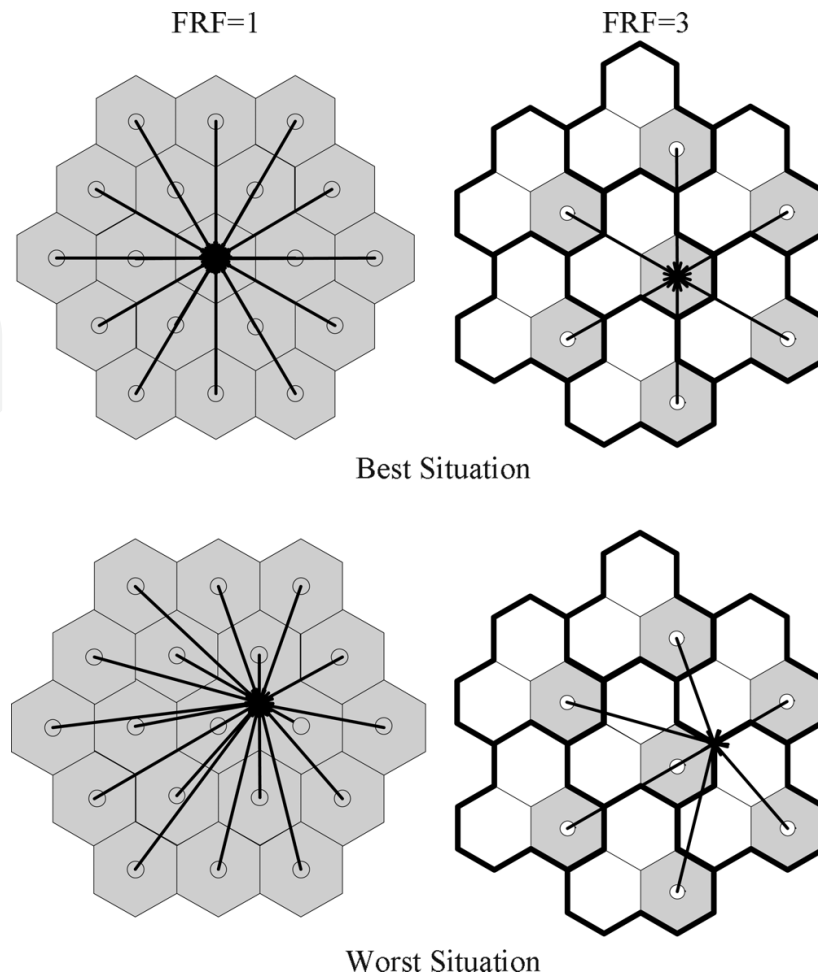
Fig. 1. Co-channel interference with integer FRFs.

interferers in both the first and second tiers will be considered. The signal-to-interference-plus-noise-ratio (SINR) at the MS is approximated by [11]

$$
\Gamma_{inte,K} \approx \begin{cases} \dfrac{P_t \cdot r_0^{-\alpha} \big/ \sigma^2 \cdot \varepsilon^{-\alpha}}{P_t \cdot r_0^{-\alpha} \big/ \sigma^2 \cdot \left[\displaystyle\sum_{i=1}^{6} \left(\dfrac{d_{K,1,i}}{r_0} \right)^{-\alpha} + \sum_{i=1}^{12} \left(\dfrac{d_{K,2,i}}{r_0} \right)^{-\alpha} \right] + 1}, K = 1 \\[2em] \dfrac{P_t \cdot r_0^{-\alpha} \big/ \sigma^2 \cdot \varepsilon^{-\alpha}}{P_t \cdot r_0^{-\alpha} \big/ \sigma^2 \displaystyle\sum_{i=1}^{6} \left(\dfrac{d_{K,1,i}}{r_0} \right)^{-\alpha} + 1}, K \geq 1 \end{cases}
$$ (12)

where r_0 is the cell radius, $\varepsilon = d_0 / r_0$ is the normalized distance between the MS and the desired BS; $d_{K,l,i}$ represents the distance between the MS and the ith co-channel BS in the $l^{th} (l = 1, 2)$ tier when the FRF equals to K. Note that the SINR expression in (12) can be used for the MS at arbitrary positions within a cell.

b.   Frequency Reuse Scheme with Non-integer FRF

In this situation, the frequencies are allocated in a more sophisticated way. Here two non-integer FRFs, 7/3 and 7/4 (following the definitions in [12]), are considered. The corresponding frequency allocation schemes are shown in Fig. 2 where symbols *f*1, …, *f*7
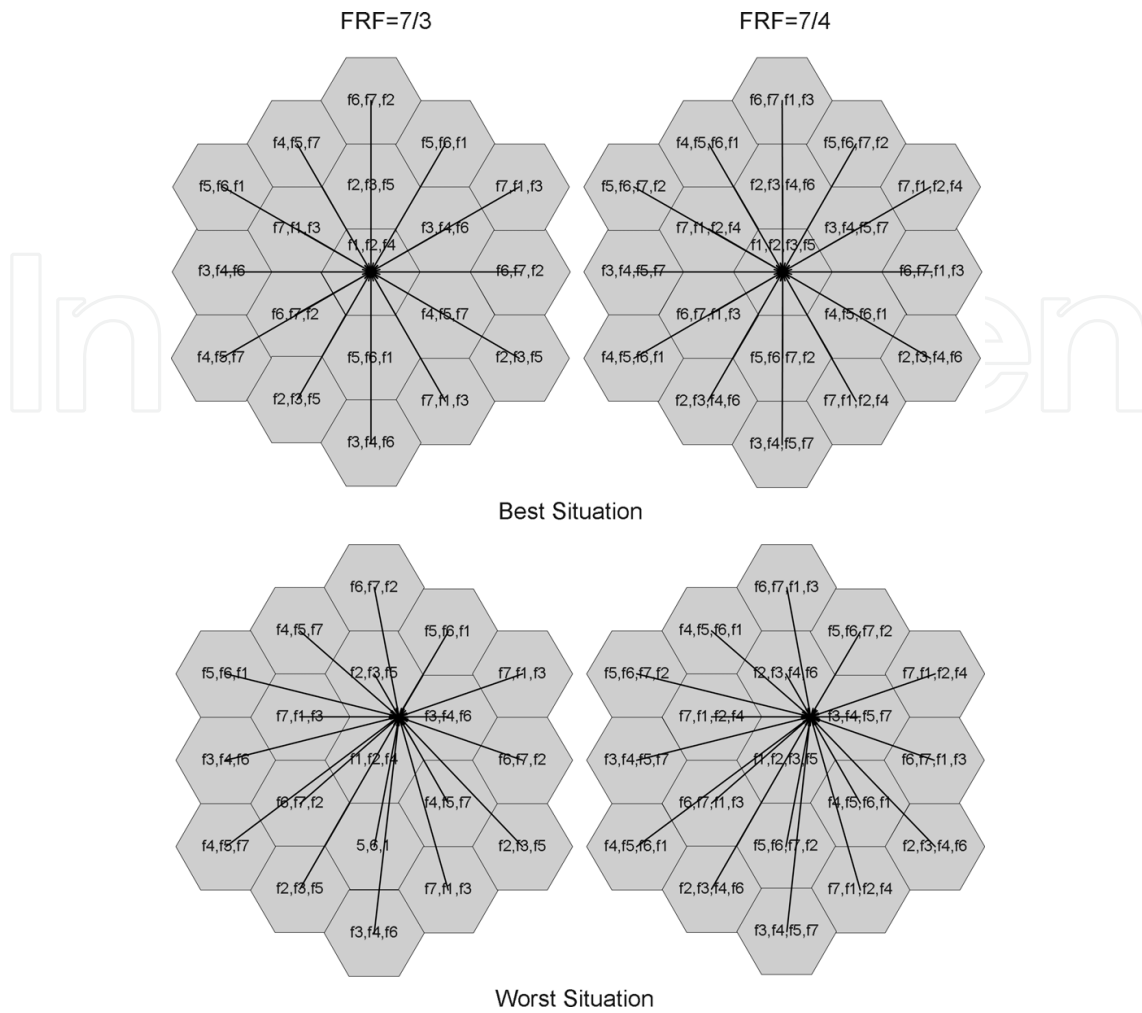
Fig. 2. Co-channel interference with non-integer FRFs.

represent the frequencies used in each cell. Take FRF=7/3 as an example. The frequency set $\{f1, f2, f4\}$ is used by the desired BS in the center. The neighboring cells use the frequency sets $\{f2, f3, f5\}$, $\{f3, f4, f6\}$, $\{f4, f5, f7\}$, $\{f5, f6, f1\}$, $\{f6, f7, f2\}$ and $\{f7, f1, f3\}$, respectively. As a result, each neighboring BS uses one frequency in common with the desired BS. Therefore, when non-integer FRF is used, the considered co-channel interferers are located similarly to the situation when FRF=1. However, the power of the interference is different. The SINR at the MS is approximated by

$$\Gamma_{non-inte,K} \approx \frac{P_t \cdot r_0^{-\alpha}/\sigma^2 \cdot \varepsilon^{-\alpha}}{\eta_K P_t \cdot r_0^{-\alpha}/\sigma^2 \cdot \left[\sum_{i=1}^{6}\left(\dfrac{d_{K,1,i}}{r_0}\right)^{-\alpha} + \sum_{i=1}^{12}\left(\dfrac{d_{K,2,i}}{r_0}\right)^{-\alpha}\right] + 1}, K \text{ is non-integer}, \quad (13)$$

where η_K is determined by the FRF K; $\eta_{7/3} = 1/3$ and $\eta_{7/4} = 1/2$.

C. Capacity analysis for cellular MIMO systems

The capacities in (7) and (8) for point-to-point MIMO systems should be modified accordingly to calculate their counterparts in cellular environment. In addition, the

capacities for an MS in the cellular environment should be normalized by the total bandwidth. Therefore, the ergodic and outage capacities are given as

$$C_K \approx \frac{1}{K}\int_0^\infty \log_2\left(1+\frac{\Gamma_K}{N_t}\lambda\right)\sum_{k=0}^{N_t-1}\left[L_k(\lambda)\right]^2 e^{-\lambda}d\lambda, \tag{14}$$

$$C_{out\%,K} \approx \frac{1}{K}m\log_2\left(1+\frac{\Gamma_K}{N_t}\lambda_{out\%}\right). \tag{15}$$

where $\Gamma_K = \Gamma_{\text{int}e,K}$ when K is integer and $\Gamma_K = \Gamma_{non-\text{int}e,K}$ otherwise; $C_{out\%,K}$ represents the outage capacity with an outage of $out\%$ when FRF $=K$ and $\lambda_{out\%}$ satisfies $P(\lambda < \lambda_{out\%}) = out\%$.

Calculating from (14) and (15), the best situation and the worst situation capacities are shown in Fig. 3 and Fig. 4 respectively. The parameters used to generate the results are as follows. The number of antennas ($N_t = N_r$) is set to be 4; the received SNR at the boundary ($P_t \cdot r_0^{-\alpha}/\sigma^2$) is set as $\{0dB,10dB,20dB,30dB\}$; the path loss exponent α is set as $\{2.5,3.5\}$; the path loss from the cell center to the cell boundary is set as -15dB (i.e., the cell radius is 3.98 km when α equals to 2.5 and 2.68 km when α equals 3.5); Finally, the FRFs are set as $\{1,7/4,7/3,3,4,7\}$.

When considering the best situation, it can be observed from Fig. 3 that:

1. The greatest ergodic capacity is achieved by the single-frequency-reuse systems. This observation also coincides with the conclusions in [15].
2. The greatest outage capacity ($C_{10\%}$) is achieved by systems using FRF=7/4 or integer FRF=3.

When considering the worst situation, it can be observed from Fig. 4 that:

1. The greatest ergodic capacity is achieved by systems using FRF=3.
2. For low and moderate values of $P_t \cdot r_0^{-\alpha}/\sigma^2$ (0 dB or 10 dB), the greatest outage capacity ($C_{10\%}$) is achieved by systems using FRF=3.
3. For higher $P_t \cdot r_0^{-\alpha}/\sigma^2$ (20 dB or 30 dB), even greater outage capacities can be obtained by using FRFs > 3. However, the increase is insignificant.

Therefore, considering the ergodic/outage capacities under best/worst situations as a whole, the optimal capacity performance may be achieved by using FRF=1, 7/4 or 3.

4. Hybrid frequency reuse scheme for cellular MIMO systems

The widely accepted approach to design the FRF is to use a fixed FRF within the entire cell. However, from the results in Fig. 3 and Fig. 4, it is obvious that a fixed FRF cannot guarantee the greatest capacities in different circumstances. For example, $K = 1$ is the optimal FRF when the MS is at the center of the cell, but it cannot support high capacity for the MSs at the cell boundary; On the other hand, $K = 3$ is a good choice when the MS is at the cell boundary. However, it cannot support high capacity for the MSs near the center of the cell. Enlightened by hybrid frequency reuse scheme for cellular SISO systems in [12], we propose a hybrid frequency reuse scheme for the cellular MIMO systems. In this hybrid frequency reuse scheme, both FRF 1 and FRF 3 will be used and adaptively allocated. One possible solution to realize the hybrid frequency reuse scheme is shown in Fig. 5 where all
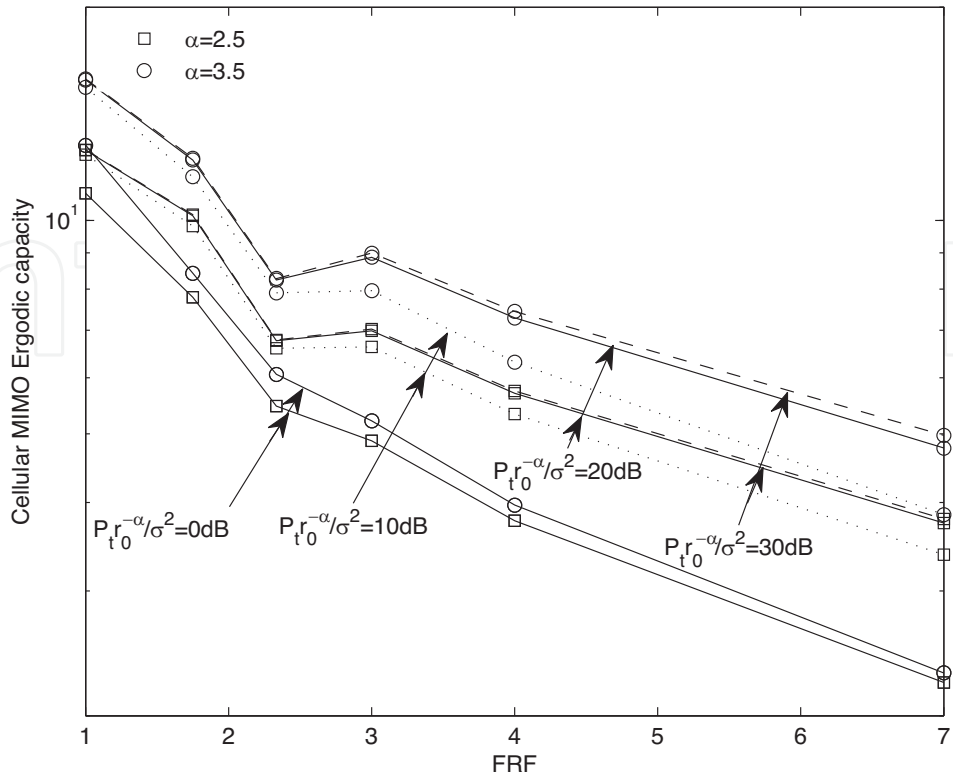
(a)
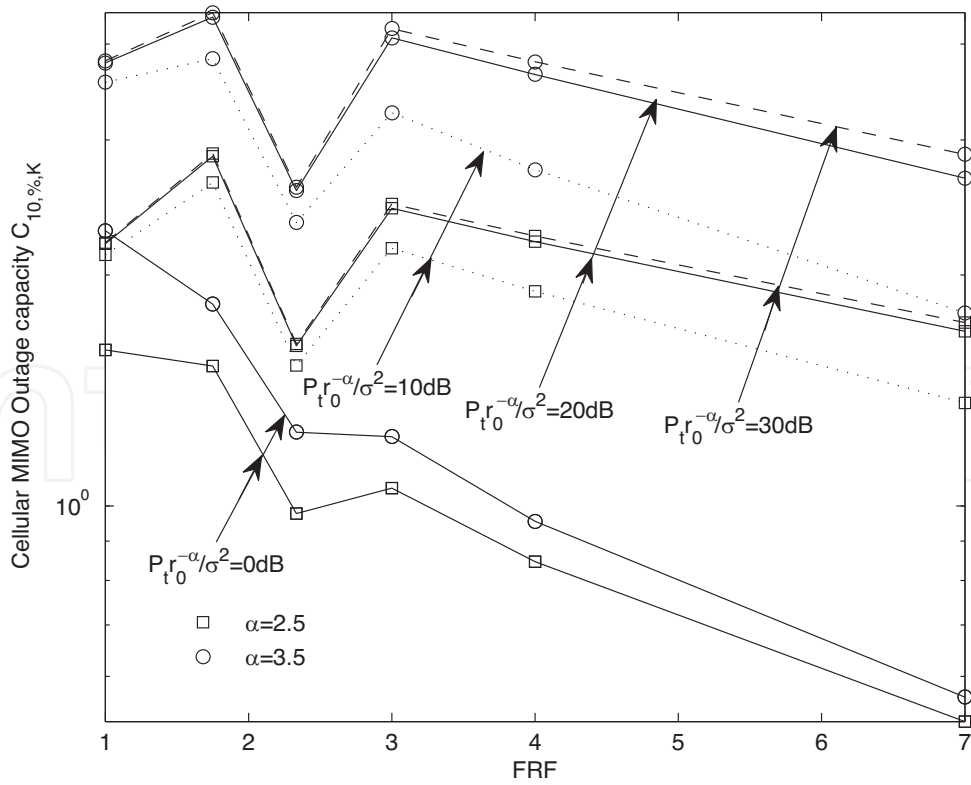
(b)

Fig. 3. Capacities of cellular MIMO systems under the best situation.
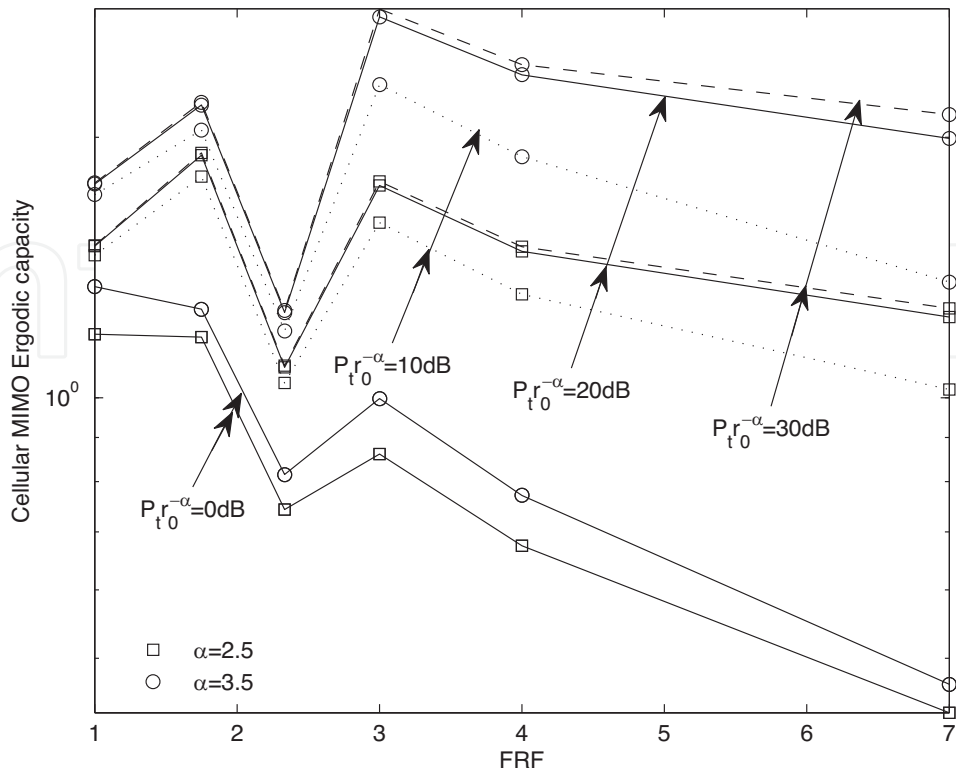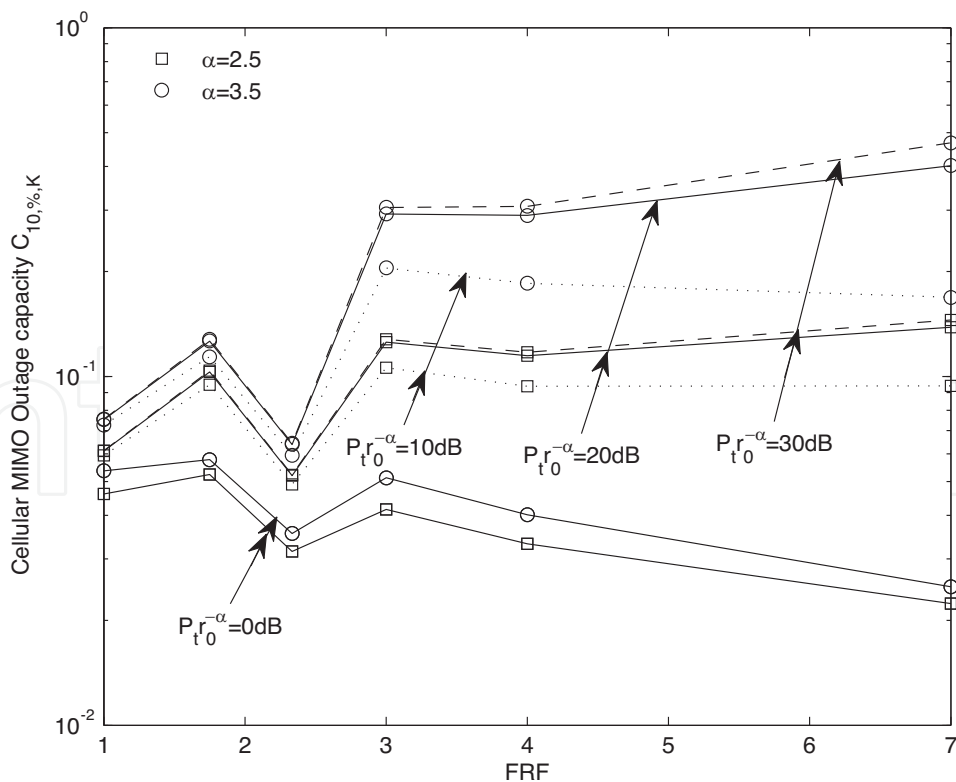
Fig. 4. Capacities of cellular MIMO systems under the worst situation.

the BSs use a frequency set of three frequencies $\{f_1, f_2, f_3\}$. For each MS, FRF 1 or FRF 3 will be used according to its position within the cell. When the MS is near the cell center, $\{f_1, f_2, f_3\}$ will all be used (FRF=1). Otherwise, when the MS is near the cell boundary, only one frequency, f_1 or f_2 or f_3, will be used (FRF=3).
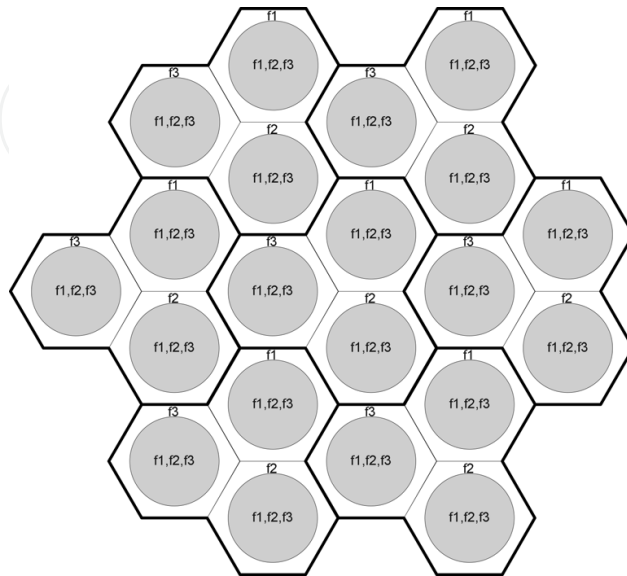

Fig. 5. Hybrid frequency reuse scheme. When the MS is near the center, three frequencies {f_1, f_2, f_3 } will be used(FRF=1); When the MS is near the boundary, only one frequency will be used (FRF=3).

For a given MS, we have determined the FRF by the following steps:

Step 1.   As the pre-knowledge, the cell radius r_0, the path loss exponent α, the transmitted power P_t and the variance of the noise σ^2 should be estimated.

Step 2.   For a given MS, estimate its distances to the desired MS d_0 and the co-channel MSs d_i, $i = 1, \cdots, B$.

Step 3.   Calculate the SINR by (12) and then evaluate the system capacities by substituting the SINR into (14) /(15) to get the ergodic/outage capacities. The capacities for $K = 1$ and $K = 3$ will be calculated respectively to get $C_1 / C_{out,1}$ and $C_3 / C_{out,3}$.

Step 4.   Select FRF so that $K = \max_K \{C_K\}$ for maximum ergodic capacity or $K = \max_K \{C_{out,K}\}$ for maximum outage capacity.

Following these steps, the FRF allocation within a cell is shown in Fig. 6 as an example where polar coordinate is used. In the figure, the hexagonal areas represent one cell, the circle areas within each cell are the areas where FRF 1 will be used. Otherwise, FRF 3 will be used. It is observed from Fig. 6 that:

1.   The FRF 1 areas shrink slightly as the path loss exponent increases.

2.   The FRF 1 areas shrink as the received SNR at the cell boundary ($P_t \cdot r_0^{-\alpha} / \sigma^2$) increases.

It is indicated that the co-channel interference problem cannot be alleviated by increasing the transmit power if single-frequency-reuse scheme is employed. Therefore, for the areas near the cell boundary, the proposed hybrid frequency reuse scheme will be a good solution to reduce the co-channel interference.
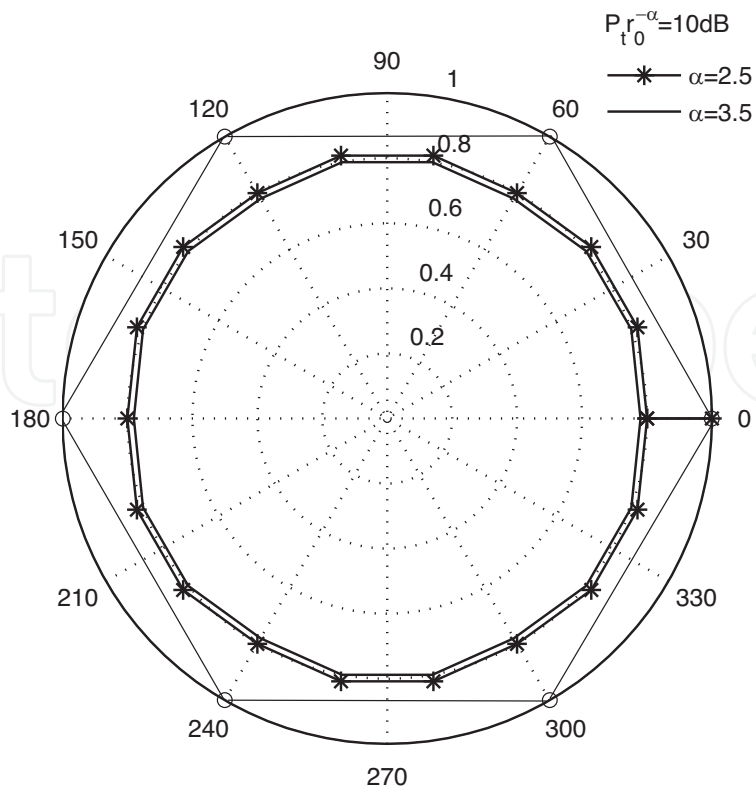
(a)
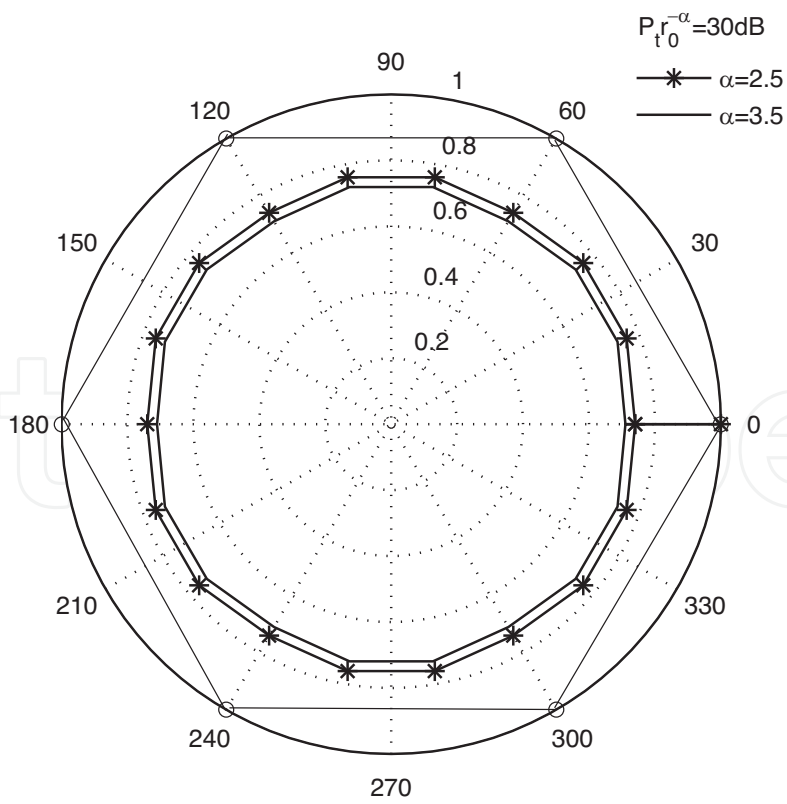
(b)

Fig. 6. FRF allocation within a cell.

5. Numerical results

It is assumed that the MS is uniformly located within a cell. The average capacities can then be calculated by averaging (14) and (15) over the entire cell. The parameters used to generate the numerical results are listed in Table I.

The capacities of cellular MIMO systems using the proposed hybrid frequency reuse scheme (hybrid FRF) are compared with those using FRF 1 and FRF 3 schemes in Fig. 7 and Fig. 8. It can be observed from that the proposed hybrid frequency reuse scheme can increase both the average ergodic and outage capacities. When compared with the FRF 1 scheme, the increase is mainly on the average outage capacities as shown in Fig. 7. The increase can be as significant as about 50% when $P_t \cdot r_0^{-\alpha}/\sigma^2$ =30 dB for the MS equipped with 8 antennas. Even for the noisy environment when $P_t \cdot r_0^{-\alpha}/\sigma^2$ =10 dB, such increase is more than 10% for the MS equipped with 2 antennas. On the other hand, when compared with the FRF 3 scheme, the increase is mainly on the average ergodic capacities as shown in Fig. 8. The increase is over 60% when $P_t \cdot r_0^{-\alpha}/\sigma^2$ =10 dB and over 47% when $P_t \cdot r_0^{-\alpha}/\sigma^2$ =30 dB.

To make it clearer, the increase of average capacities gained by the hybrid FRF over the FRF 1 scheme and FRF 3 scheme is summarized in Table II in percentage.

Number of antennas ($N_t = N_r$)	2~8
Received SNR at the cell boundary $P_t \cdot r_0^{-\alpha}/\sigma^2$	10dB, 30dB
Path loss exponent α	3.5
Path loss from the cell center to the cell boundary	-15dB
Frequency allocation schemes	FRF1, FRF 3, proposed hybrid frequency reuse scheme

Table I. Parameters

			Number of antennas						
			2	3	4	5	6	7	8
Over FRF 1	Outage	$P_t \cdot r_0^{-\alpha}/\sigma^2 = 10dB$	10.5%	12.8%	14.3%	15.3%	16.7%	17.5%	17.8%
		$P_t \cdot r_0^{-\alpha}/\sigma^2 = 30dB$	21.7%	29.8%	37.8%	43.7%	47.4%	49.5%	49.9%
	Ergodic	$P_t \cdot r_0^{-\alpha}/\sigma^2 = 10dB$	1.6%	1.6%	1.6%	1.6%	1.6%	1.6%	1.6%
		$P_t \cdot r_0^{-\alpha}/\sigma^2 = 30dB$	3.0%	3.0%	3.0%	3.0%	3.0%	3.0%	3.0%
Over FRF 3	Outage	$P_t \cdot r_0^{-\alpha}/\sigma^2 = 10dB$	13.6%	7.6%	3.8%	1.4%	0.5%	0.1%	-*
		$P_t \cdot r_0^{-\alpha}/\sigma^2 = 30dB$	2.9%	-	-	-	-	-	-
	Ergodic	$P_t \cdot r_0^{-\alpha}/\sigma^2 = 10dB$	62.9%	63.1%	63.4%	63.5%	63.6%	63.7%	63.7%
		$P_t \cdot r_0^{-\alpha}/\sigma^2 = 30dB$	47.3%	47.6%	47.8%	47.9%	48.0%	48.1%	48.1%

*represents no increase

Table II. The increase of average capacities of the proposed hybrid frequency reuse scheme
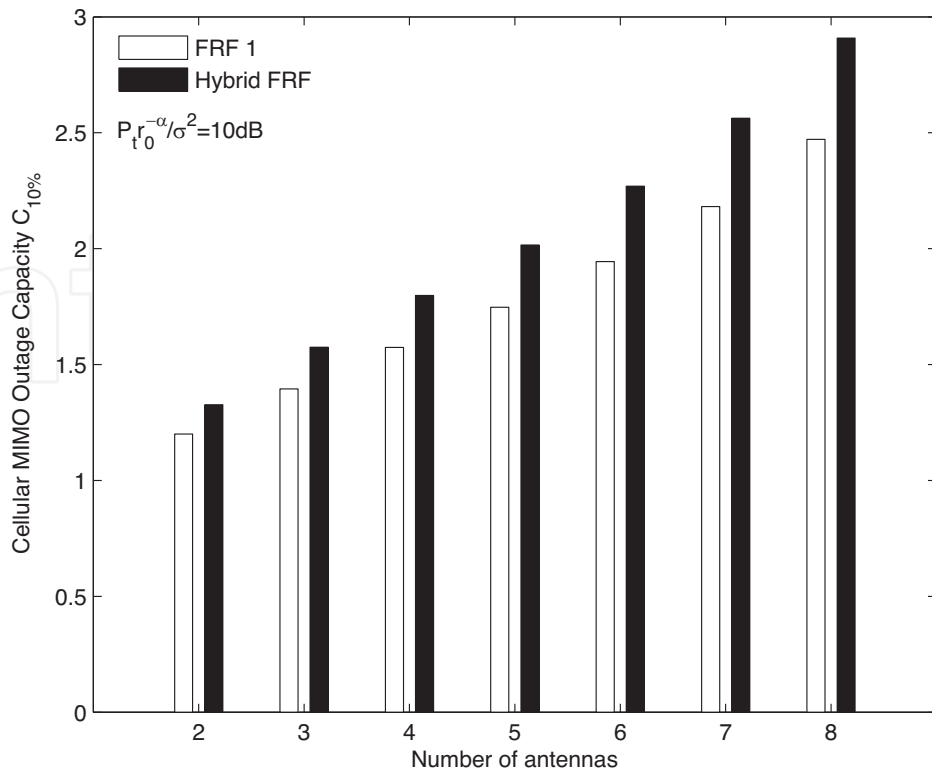
(a)
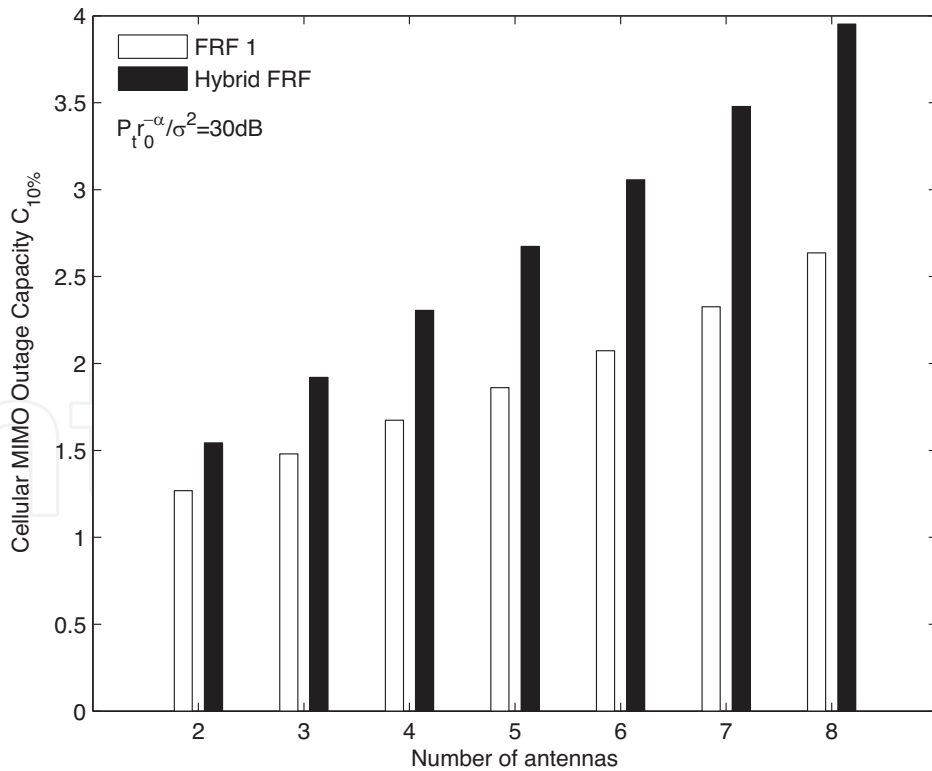
(b)

Fig. 7. Average 10% outage capacities of the cellular MIMO systems using FRF 1 scheme and the hybrid frequency reuse scheme.
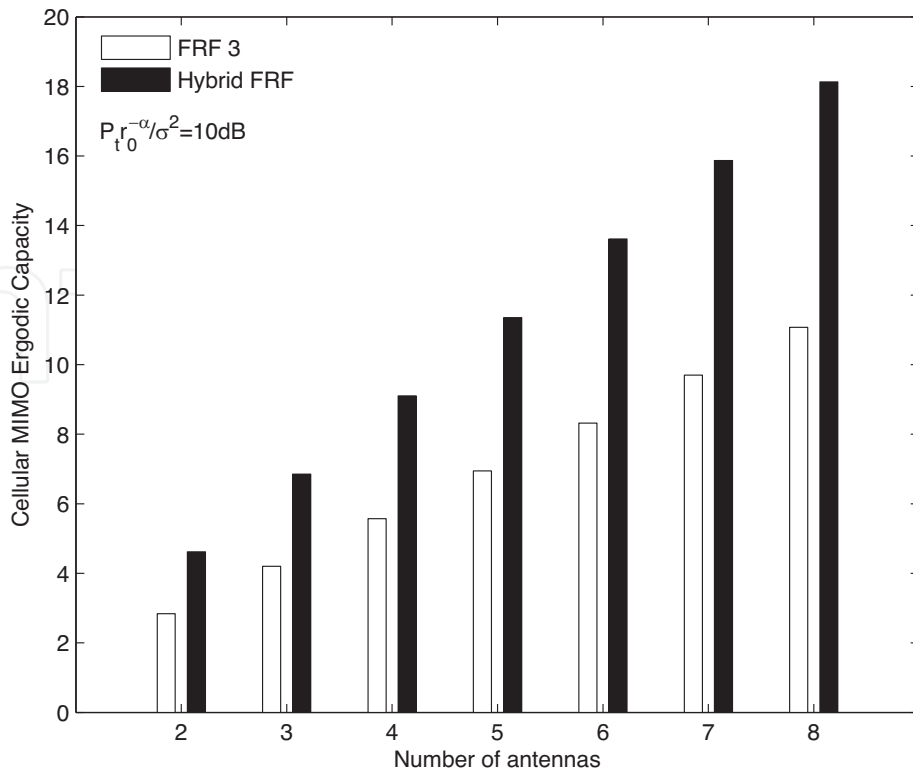
(a)
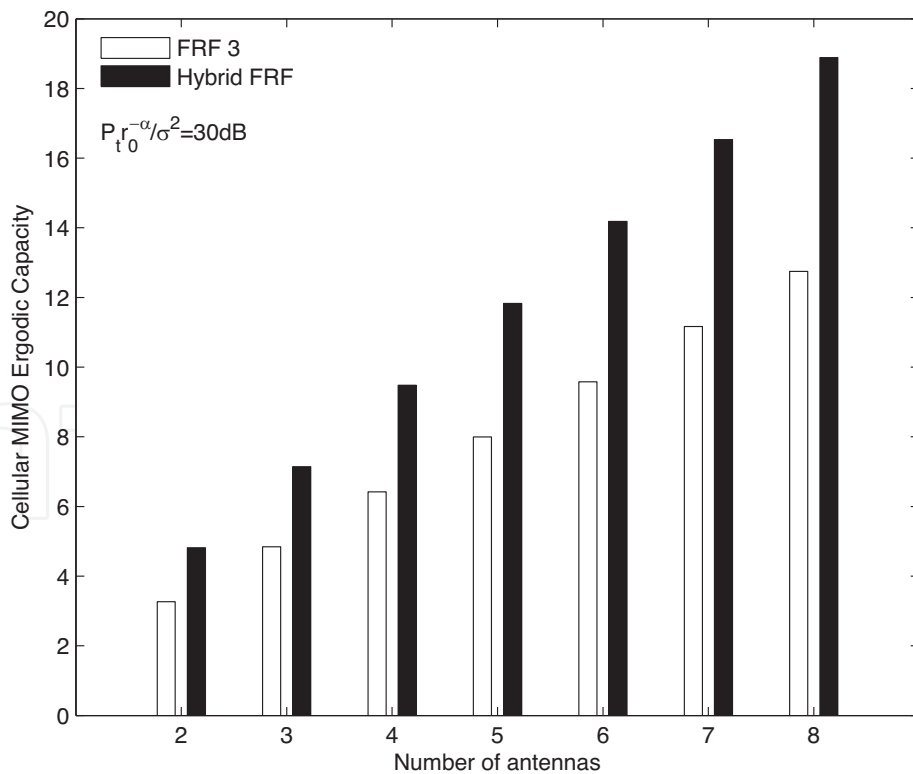
(b)

Fig. 8. Average ergodic capacities of the cellular MIMO systems using FRF 3 scheme and the hybrid frequency reuse scheme.

Remark: As we know, the coverage problem (the transmission between the BS and MS fails at the cell boundary due to the co-channel interference) has been the major problem for the commonly used single-frequency-reuse cellular systems. From the numerical results, it is seen that such problem can be greatly alleviated by using the proposed hybrid frequency reuse scheme.

6. Conclusions

In this chapter, the downlink capacity of cellular MIMO systems has been theoretically analyzed in terms of both ergodic and outage capacities. The FRF has been considered and a hybrid frequency reuse scheme has been introduced. Numerical results have shown that both the ergodic and outage capacities can be increased by the hybrid FRF scheme. Especially, when compared with the commonly used FRF 1 scheme, the outage capacity can be increased as much as 50%. Therefore, the hybrid FRF scheme can greatly alleviate the coverage problem of the single-frequency-reuse cellular systems.

7. Reference

[1] V. Tarokh, N. Sehadri and A. R. Calderband, "Space-time codes for high data rate wireless communication: Performance criterion and code constructions," IEEE Transactions on Information Theory, vol. 44, pp. 744-765, March 1998.

[2] G. J. Foschini, "Layered space-time architecture for wireless communication in a fading environment when using multielement antennas," Bell Labs Technical Journal, pp. 41-59, Autumn 1996.

[3] G. J. Foschini and M. J. Gans, "On limits of wireless communications in a fading environment when using multiple antennas," Wireless Personal Communications, vol. 6, pp. 311-335, 1998.

[4] E. Telatar, "Capacity of multi-antenna Gaussian channels," European Transactions on Telecommunications, vol. 10, pp. 585-595, November 1999.

[5] M. S. Alouini and A. J. Goldensmith, "Area spectral efficiency of cellular mobile radio systems," IEEE Transactions on Vehicular Technology, vol. 48, pp. 1047-1066, July 1999.

[6] R. S. Blum, J. H. Winters and N. R. Sollenberger, "On the capacity of cellular systems with MIMO," IEEE Communications Letters, vol. 6, pp. 242-244, June 2002.

[7] W. Matthew, B. Mark and N. Andrew, "Capacity limits of MIMO channels with co-channel interference," IEEE Vehicular Technology Conference, pp. 703-707, 2004.

[8] M. M. Matalgah, J. Qaddour, A. Sharma and K. Sheikh, "Throughput and spectral efficiency analysis in 3G FDD WCDMA cellular systems," IEEE Globecom conference, pp. 3423-3426, November 2003.

[9] S. Catreux, P. F. Driessen and L. J. Greenstein, "Simulation results for an interference-limited multiple-input multiple-output cellular sysem," IEEE Communications Letters, vol. 4, pp. 334-336, November 2000.

[10] S. Catreux, P. F. Driessen and L. J. Greenstein, "Attainable throughput of an interference-limited Multiple-Input Multiple-Output (MIMO) cellular systems ," IEEE Transactions on Communications, vol. 49, pp. 1307-1311, August 2001.

[11] K. Adachi, F. Adachi and M. Nakagawa, "On cellular MIMO spectrum efficiency," IEEE Vehicular Technology Conference, pp. 417-421, October 2007.

[12] Y. J. Choi, C. S. Kim and S. Bahk, "Flexible design of frequency reuse factor in OFCDM cellular networks," IEEE International Conference on Communications, pp. 1784-1788, May 2006.
[13] T. M. Cover and J. A. Thomas, Elements of information theory, New York: Wiley, 1991.
[14] J. G. Proakis, Digital Communications, New York: McGraw Hill, 2001.
[15] Z. Wang and R. S. Gallacher, "Frequency reuse scheme for cellular OFDM systems," IEEE Electronics Letters, vol. 38, pp. 387-388, April 2002.
[16] Wei Peng and Fumiyuki Adachi, "Hybrid Frequency Reuse Scheme for Cellular MIMO Systems," IEICE Transactions on Communications, vol. E92-B, May 2009.
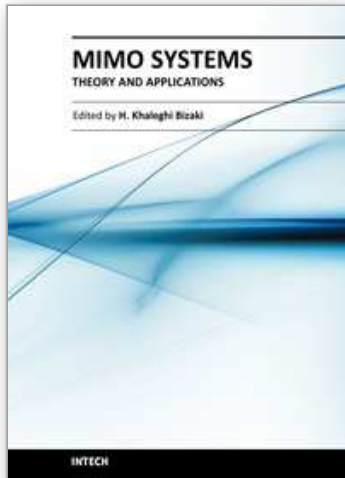
MIMO Systems, Theory and Applications

Edited by Dr. Hossein Khaleghi Bizaki

In recent years, it was realized that the MIMO communication systems seems to be inevitable in accelerated evolution of high data rates applications due to their potential to dramatically increase the spectral efficiency and simultaneously sending individual information to the corresponding users in wireless systems. This book, intends to provide highlights of the current research topics in the field of MIMO system, to offer a snapshot of the recent advances and major issues faced today by the researchers in the MIMO related areas. The book is written by specialists working in universities and research centers all over the world to cover the fundamental principles and main advanced topics on high data rates wireless communications systems over MIMO channels. Moreover, the book has the advantage of providing a collection of applications that are completely independent and self-contained; thus, the interested reader can choose any chapter and skip to another without losing continuity.

How to reference

In order to correctly reference this scholarly work, feel free to copy and paste the following:

Wei Peng (2011). Cellular MIMO Systems, MIMO Systems, Theory and Applications, Dr. Hossein Khaleghi Bizaki (Ed.), ISBN: 978-953-307-245-6, InTech, Available from: http://www.intechopen.com/books/mimo-systems-theory-and-applications/cellular-mimo-systems

INTECH
open science | open minds